DESIGN OF EQUIPMENT FOR DETERMINING SUSPENSION CHARACTERISTICS OF HEAVY VEHICLES

AUG. 1963
NO. 21

Joint Highway Research Project

PURDUE UNIVERSITY
LAFAYETTE INDIANA

by

J. W. McLemore

Final Report

DESIGN OF EQUIPMENT FOR DETERMINING SUSPENSION CHARACTERISTICS

OF HEAVY VEHICLES

TO: K. B. Woods, Director
Joint Highway Research Project

August 2, 1963

FROM: H. L. Michael, Associate Director
Joint Highway Research Project

File: 6-20-6
Project No: C-36-52F

Attached is a report entitled "Design of Equipment for Determining Suspension Characteristics of Heavy Vehicles" by Mr. James W. McLemore, Graduate Assistant on our staff. The research reported has been performed under the direction of Professor B. E. Quinn of the School of Mechanical Engineering. Mr. McLemore also used this research for the thesis requirements for an MSME degree.

This research was performed as part of the "Stresses and Deflections" HPS research project and is submitted as a progress report of that research. This study was performed as part of the preliminary phase of this research to develop a device for measuring the tire force of a moving truck. The success of this study was one of the factors which permitted the early proposal for the expansion of the "Stresses and Deflections" project and was one of the primary purposes of the pre-investigation phase of this research.

The report is presented for the record and will be submitted to the Indiana State Highway Commission and the Bureau of Public Roads for their review and comments.

Respectfully submitted,

H. L. Michael
Associate Director

HLM:bc

Attachments

Copy: F. L. Ashbuacher
J. R. Cooper
W. L. Dolch
W. H. Goetz
F. F. Havey
F. S. Hill
G. A. Leonards
J. F. McLaughlin
R. D. Miles
R. E. Mills
M. B. Scott
J. V. Smythe
E. J. Yoder

Final Report

DESIGN OF EQUIPMENT FOR DETERMINING SUSPENSION OF HEAVY VEHICLES

by

James Wilson McLemore
Graduate Student

Joint Highway Research Project

File No: 6-20-6

Project No: C-36-52F

Prepared as Part of an Investigation

Conducted by

Joint Highway Research Project
Engineering Experiment Station
Purdue University

in cooperation with

Indiana State Highway Commission

and the

Bureau of Public Roads
U S Department of Commerce

Not Released for Publication

Subject to Change

Not Reviewed By

Indiana State Highway Commission
or the
Bureau of Public Roads

Purdue University
Lafayette, Indiana
October 31, 1963

Final report

Impact of Economic and Institutional Environment on Export Decision

by

James Wilson Rodgers
Professor Economics

Florida Technology Executive Institute

Orlando, Florida

August 20, 1990

Prepared on Grant #1 for Contemporary

Commerce, Inc.

Florida Technology Executive Institute
Contemporary Development Authority
Florida Technology

In cooperation with

Commerce Office Systems Consulting

and the

Bureau of Business Trends
U.S. Department of Commerce

ACKNOWLEDGMENTS

The author wishes to acknowledge the assistance obtained from previous developmental work performed under Contract CPR11-7941 with the Bureau of Public Roads and for some financial assistance provided by that contract in the design of the equipment reported herein. Future work under that contract will also use the equipment here reported.

Several individuals had a direct influence on the design of the equipment described in this thesis. The author wishes to express his most sincere appreciation to Dr. Bayard E. Quinn, Professor of Mechanical Engineering for his supervision and advice as the major professor. Professor E. O. Stitz and Professor E. J. Yoder also contributed valuable advice in their respective fields.

The continued assistance and moral support of Mr. Clement C. Wilson helped the design over many tough spots. Mr. Jack Zable, John Bruhl, and Erling Hestad assisted with the drafting, construction, assembly and testing of many of the components.

TABLE OF CONTENTS

TABLE OF CONTENTS (continued)

LIST OF FIGURES

ABSTRACT

#21

McLemore, James Wilson, M.S.M.E., Purdue University, June, 1963. Design of Equipment for Determining Suspension Characteristics of Heavy Vehicles. Major Professor: B. E. Quinn, Ph.D.

A tire of a moving vehicle will in general exert a fluctuating force upon the pavement. This force will consist of the static wheel component of force due to motions in the vehicle suspension system that are induced by irregularities in the pavement profile. This fluctuating force component is frequently referred to as the "dynamic force" and it can be determined by measuring the fluctuations in the air pressure of the tire as the vehicle moves along the highway.

It is of course necessary to obtain the relationship between air pressure and tire force if measurements of air pressure are to be used to determine the dynamic force. This relationship can be obtained by simultaneously measuring the air pressure and the tire force as the tread of the tire is subjected to a sudden motion.

A device for doing this with trucks, referred to as a truck calibrator, is described in this report. The motion of the tread of the tire is obtained by placing a wheel of the truck in the middle of a beam that is pivoted at one end and is held in the raised position at the other end with a latch. When the latch is released the beam rotates through a very small angle and is brought suddenly to a rest. Fastened to the beam is a force-measuring transducer upon which the tire rests.

This transducer measures the force of the wheel upon the beam at all times and furnishes the force measurement previously mentioned. The air pressure measurement is made by a separate system and is not part of the calibrator.

The design of the major components of the calibrator is outlined in this report. Predicted characteristics are checked experimentally to test the validity of the design theory that is employed.

The truck calibrator is presently mounted in a pit near the Jet Propulsion Laboratory and is ready for service.

CHAPTER 1

INTRODUCTION

When a vehicle is driven over a perfectly smooth highway, it experiences no vertical motion. The vehicle body travels in pure horizontal translation as long as there are no bumps or ripples in the highway surface to cause vertical displacements.

Such an ideal highway with no surface irregularities is very rare. Most highways have some bumps or waves which cause an up-and-down motion of the vehicle body. These profile variations could be present in a newly constructed highway due to the contour of the land. In older highways these could be due to deterioration of the pavement.

A vehicle parked or moving over a "perfectly smooth" highway exerts a force on the pavement equal to the static wheel load. If vertical motions of the body are present, they cause a varying or dynamic force to be impressed upon the road in addition to the static wheel load. These dynamic forces are functions of the road profile, vehicle velocity, vehicle suspension characteristics and size of the vehicle. Generally, larger vehicles and rougher roads give rise to larger dynamic forces.

The exact effect of these dynamic forces on pavement behavior is not known. One school of thought maintains that they directly influence the wear and deterioration of the road. It is possible that varying forces could cause stress reversals in the pavement which might result in fatigue types of failure. Another school of thought contends that pavement deterioration is due principally to the adverse effects of weather. A better understanding

of the relationship between dynamic forces and highway profiles may help to explain their importance.

The research program of which this thesis was a part had two over-all objectives: They were:

1. Development of a means of predicting the dynamic forces exerted upon a specific highway as a given vehicle travels over it.
2. Development of a means of measuring the dynamic forces.

The prediction of dynamic forces has been attempted mathematically (1)*. In this approach, highway elevations were measured by a survey team. The power spectral density function was computed from these elevation measurements. This gave a frequency domain characterization of the highway profile (when the vehicle velocity was introduced) which can be thought of as a displacement input to an elastic system. A vehicle suspension system characteristic, or "transfer function" was obtained from calibration tests on the vehicle which was used. Combining these, the prediction was made of the dynamic force that would be exerted upon the highway.

Actual measurement of dynamic force has been attempted by several methods (2, 4, 5). On this project, force measurements were made by recording the variation in air pressure occurring in a tire as the vehicle traveled along the highway. The relationship between air pressure variation and variation in force on the highway was obtained by calibration tests on the vehicle. The predicted and measured values of the dynamic forces should agree. Emmerson (2) illustrated this schematically in Figure 1.

---

* Numbers refer to the bibliography.

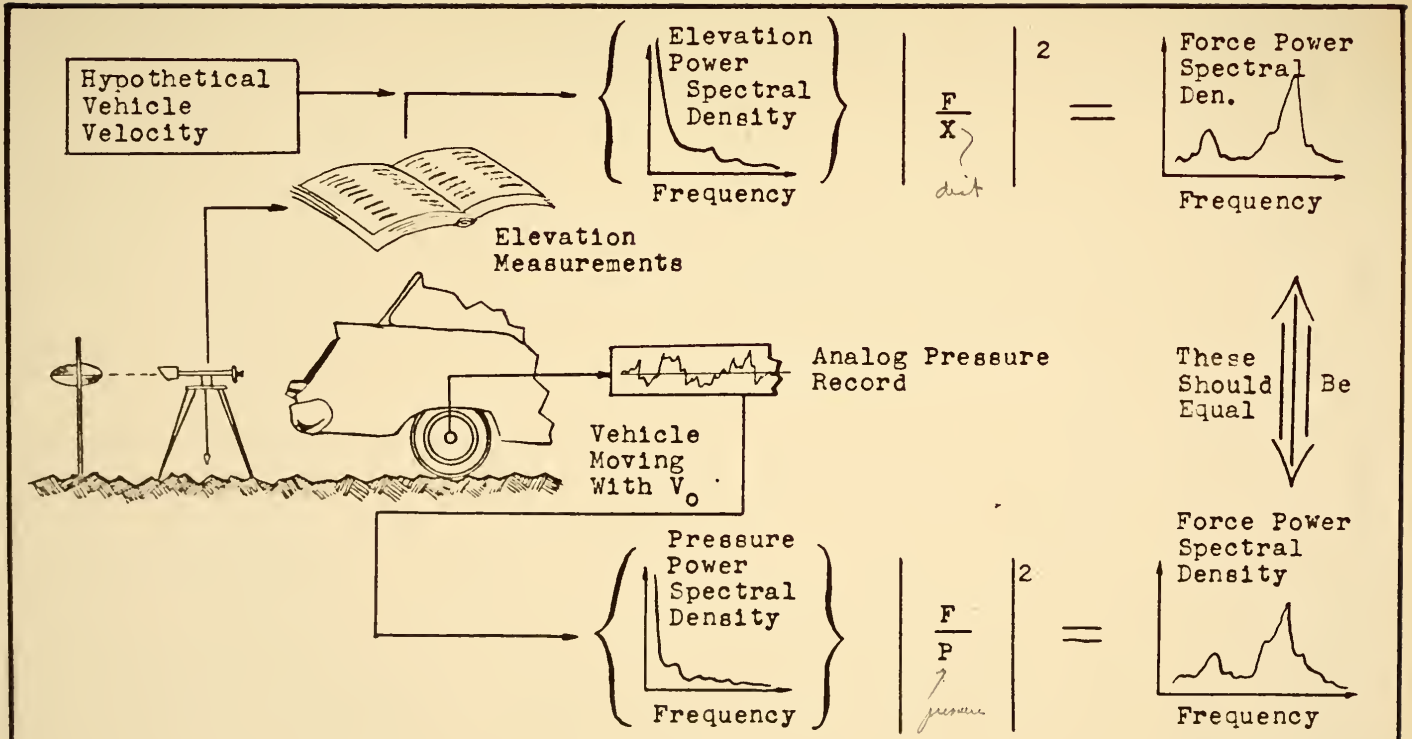

FIGURE 1 - TWO METHODS OF CALCULATING FORCE POWER SPECTRAL DENSITY FUNCTION

In both the prediction and measurement of dynamic forces, suspension characteristics of the vehicle were needed. Equipment had previously been designed to be used in the calibration of passenger vehicles (1, 3). This thesis describes the design of equipment for the calibration of trucks.

CHAPTER 2

COMPARISON OF DIFFERENT TYPES OF EQUIPMENT USED IN DETERMINATION OF SUSPENSION CHARACTERISTICS

De Vries (1) designed a steady state vibrator to be used for determining suspension system characteristics. This device gave a steady state sinusoidal displacement to the wheel of a car. The wheel was positioned on a load cell so that the variation of force of the wheel on the cell could be recorded. Air pressure variations in the tire could also be recorded. While the amplitude and frequency of the input could be varied, the input was always a pure sinusoidal motion.

Later, Hamilton (3) built a transient test device for use with passenger vehicles. This was a pivoted beam with a load cell at the center. (See Figure 2). The vehicle was driven up on the beam with one wheel resting on the load cell. The beam was then raised and dropped. This produced a step input to the wheel, or if the raising and lowering was done in one continuous motion, it gave a pulse input to the wheel. (See Figure 3). Both types of input used in the transient test seemed to have advantages over the steady state input. A harmonic analysis of the pulse and step inputs is shown in Figures 4 and 5. Both of these inputs are made up of a series of harmonics of different amplitudes and frequencies, while as mentioned previously the steady state test input was made up of only one amplitude and one frequency. For this reason, Hamilton (3) maintains that the transient test yields better results than the steady state test because the frequency content of the transient test input is more like the frequency content of the typical highway as determined by the power spectrum analysis.

FIGURE 2 : TRANSIENT TEST DEVICE FOR USE WITH PASSENGER VEHICLES

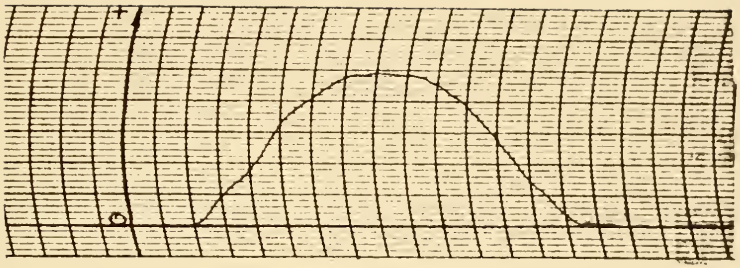

RECORD OF TYPICAL PULSE

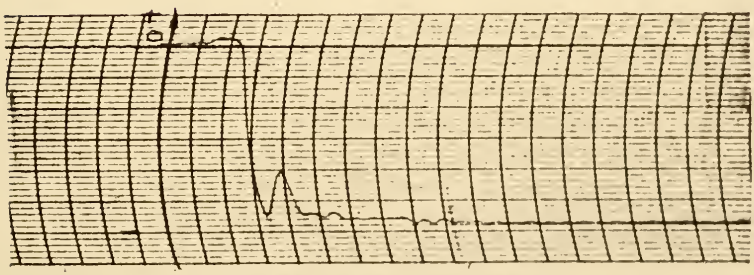

RECORD OF TYPICAL STEP INPUT

FIGURE 3

FIGURE 4: HARMONIC CONTENT OF PULSE INPUT

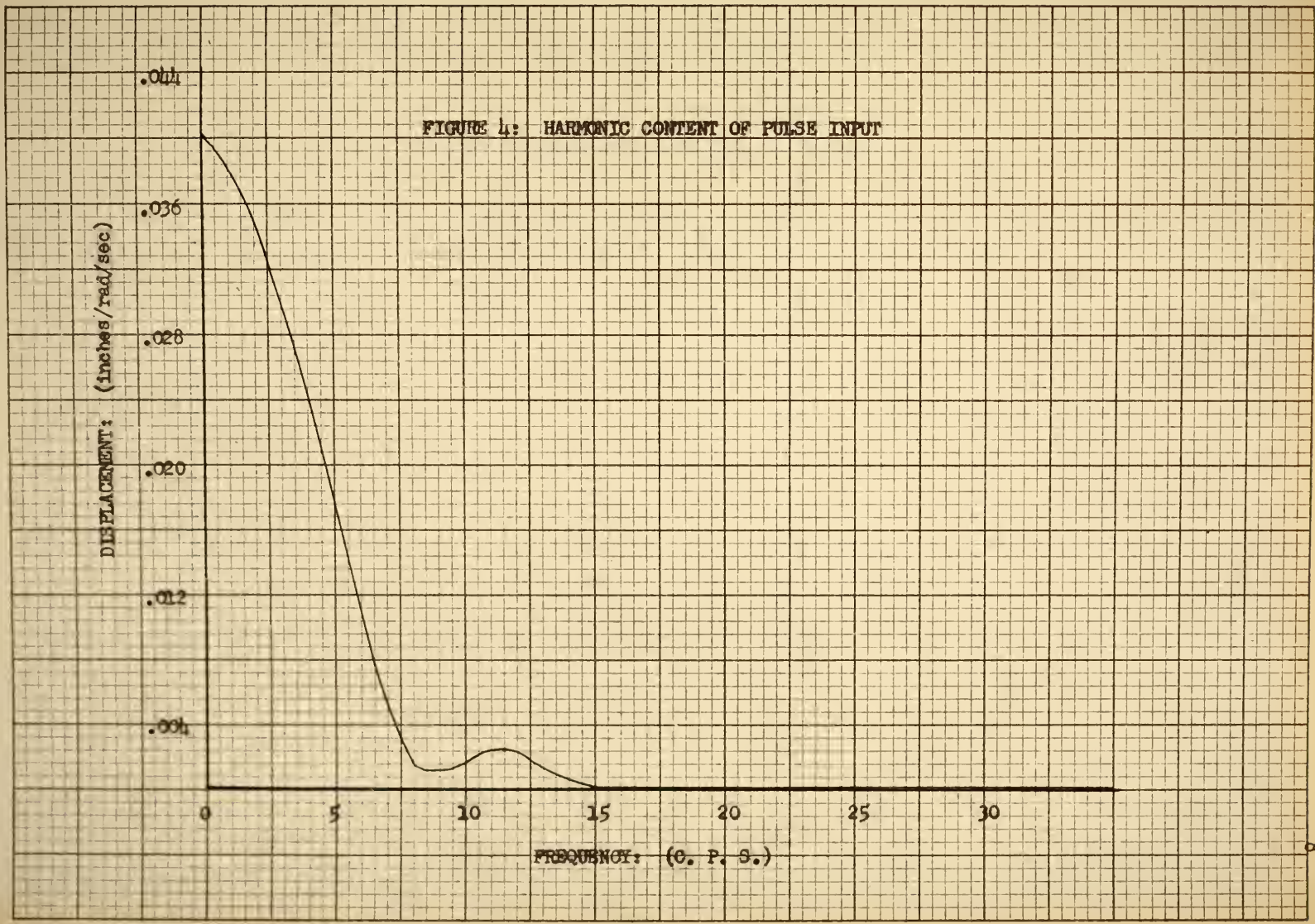

FIGURE 5: HARMONIC CONTENT OF STEP INPUT

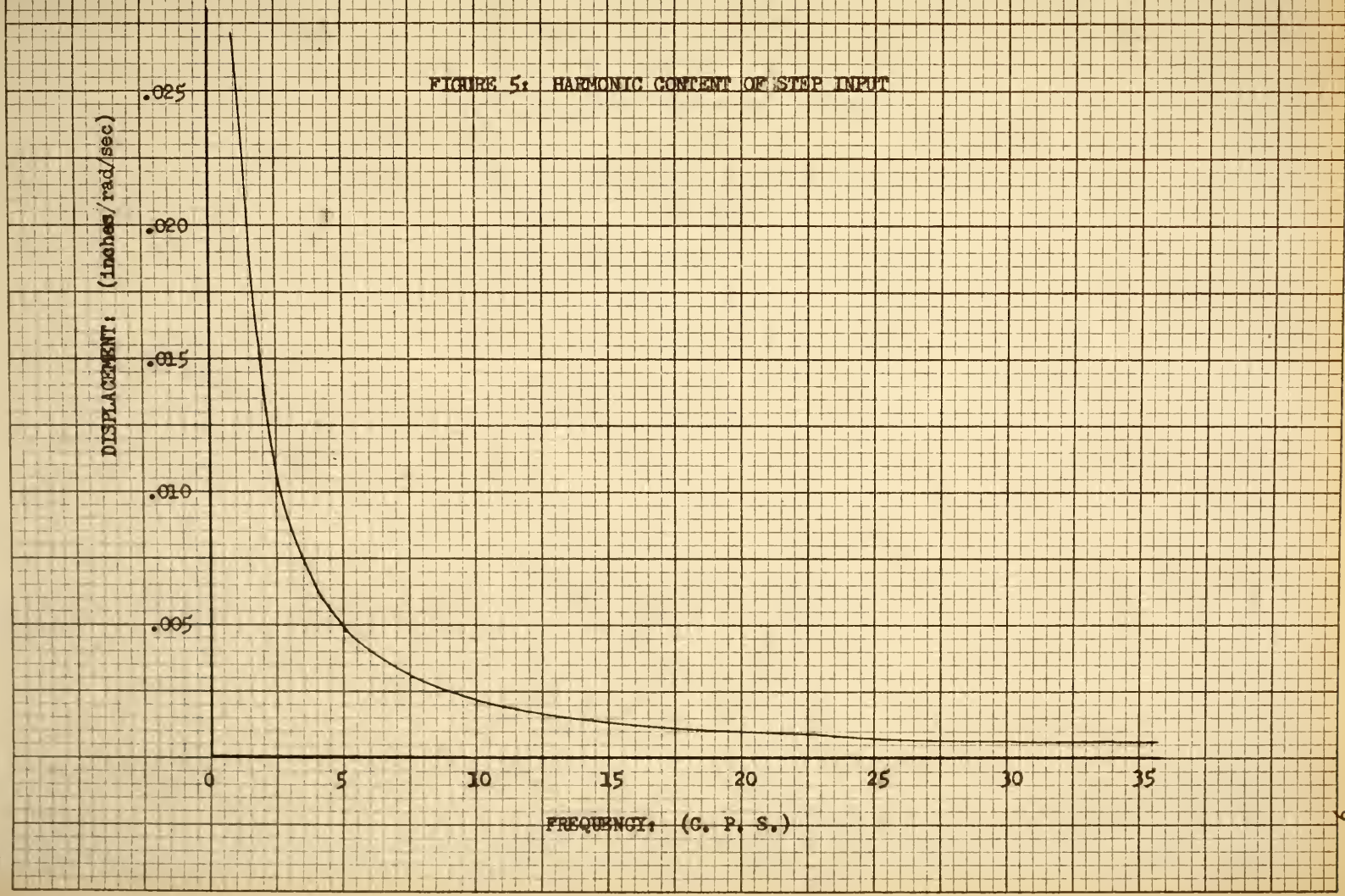

In extending De Vries' and Hamilton's work on suspension characteristics to include trucks, the increased weight makes size problems more critical. A steady state vibrator for trucks would be extremely large. Also, previous work with cars indicates that the two types of transient test inputs give similar results, and the steady state test results differed greatly from them. As mentioned above, this is probably due to the fact that the harmonic content of the transient input is more like the frequency content of the highway. For these reasons, a transient test was selected for the determination of truck suspension characteristics.

The transient test device described in this thesis is shown in Figure 6. It consists of a pivoted beam with a latch mechanism. A hydraulic jack is used to raise the beam and the latch holds it in the raised position. The latch is then tripped and the beam is dropped. With the beam as it is presently constructed, only a drop test can be obtained. It can easily be adapted, however, to produce a pulse input by the addition of a driving mechanism. If it becomes apparent that a pulse input is needed, recommendations concerning additional equipment to be used with the existing design are given in Chapter 6.

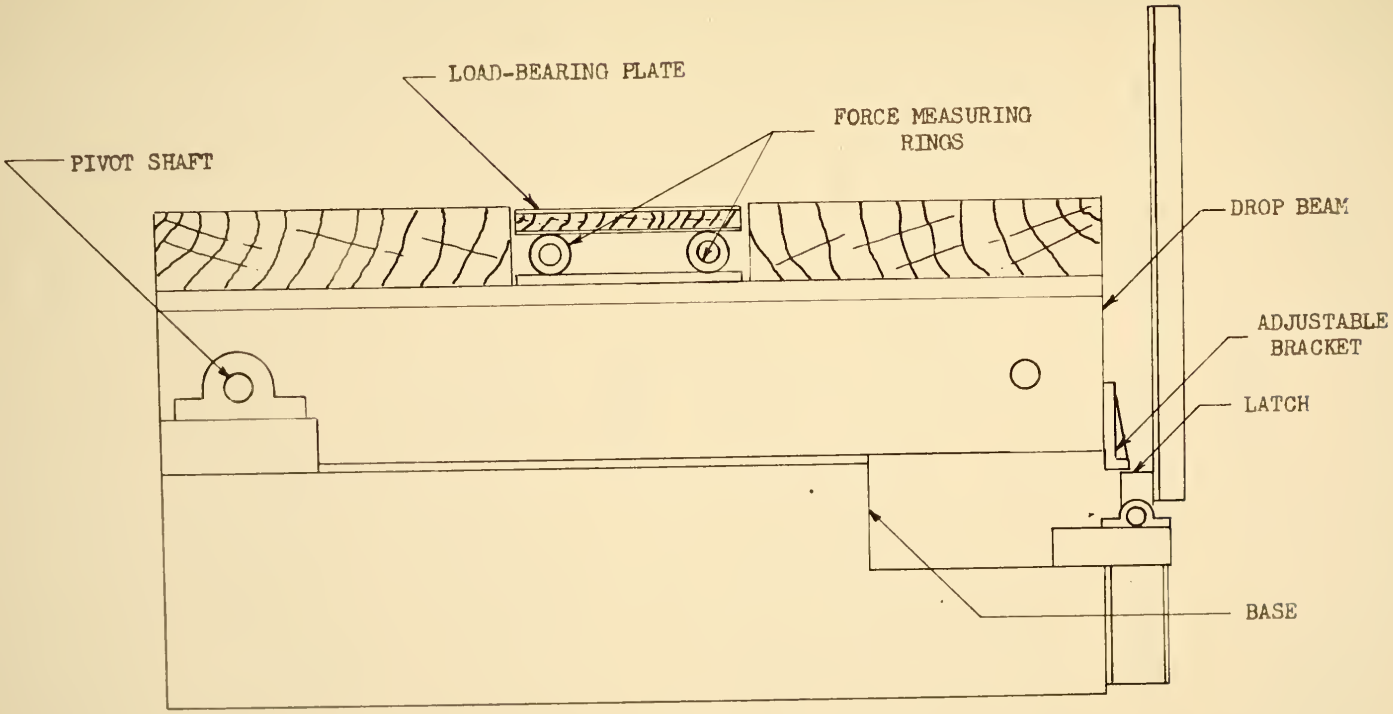

FIGURE 6: DRAWING OF TRUCK CALIBRATOR

CHAPTER 3

FACTORS INFLUENCING THE DESIGN OF THE CALIBRATOR

As stated in Chapter 2, the calibrator described in this thesis consists principally of a pivoted drop beam and a latching mechanism. Two force measuring cells are mounted on top of the beam. These consist of plates (which support the wheels) mounted on top of four cylindrical rings. Strain gages attached to the rings are calibrated to measure the force exerted upon the plate. The factors influencing the design specifications of these members can best be described by considering individually the major components of the calibrator.

Drop Beam

The legal load limit for one end of a truck axle is 9,000 pounds. However, since trucks on the highways are sometimes overloaded, the drop beam may possibly be used to calibrate overloaded trucks. For this reason, a static design load of 14,000 pounds was selected.

The drop beam must support the static load of 14,000 pounds, and also a dynamic or fluctuating load. The magnitude of the dynamic force which will be exerted by a truck on the beam is not known, but previous work (6) with passenger vehicles indicates that it might vary from approximately $\pm$ 200 pounds to $\pm$ 3,000 pounds.

Although extensive tests have been conducted on passenger vehicles in the laboratory, no comparable information has been obtained for trucks. In addition, the literature contains only scanty information (7) on the

frequency response characteristics of these vehicles. Previous work with passenger vehicles, however, made it seem unlikely that any frequencies above 30 cycles per second would be excited in a truck test. All of the natural frequencies of the loaded drop beam should be much greater than any frequency excited in the test. This condition would seemingly be met if the beam, loaded with the static wheel load of 14,000 pounds, had no natural frequencies below 50 cycles per second.

The drop beam was designed to accomodate several different conditions. First, it was made wide enough to accept a set of dual wheels. When used with duals, the force variation under each wheel can be measured separately. Secondly, it can be used to measure the force variation under a single wheel without inducing an eccentric loading in the drop beam. The two load measuring cells were built as separate modular units, making the changeover from single to dual wheels very simple.

As mentioned in Chapter 2, the beam will be raised with a jack and will be held up with a latch. Also, the beam must be as easily and economically fabricated as possible. All of these factors made it desirable for the beam to weigh as little as possible. In the completed design, the beam weighed about 600 pounds, or less than 4.5 percent of the static wheel load for which it was designed.

Load Sensing Members

The load sensing members used in the load cells could have been made in several forms. Load cells utilizing compression members as load sensors have been manufactured and sold commercially. In this particular application, however, a relatively small force fluctuation was superimposed on a large

static force. The load sensing members therefore, had to satisfy the following specifications:

1. They had to be strong enough to support the static and dynamic loads, or, the maximum stress due to the maximum static load had to be much less than the proportional limit.
2. The strains caused by the fluctuating force during the test had to be sizeable enough to measure.
3. The rings and loaded plate should have no natural frequency below 50 cycles per second.

The load sensors were made in the form of cylindrical rings because it was easier to obtain the required sensitivity with rings rather than with other types of sensing members. Steel or aluminum alloy rings could have been used, but it is shown in Chapter 4 that aluminum alloy rings provide better sensitivity.

Load-Bearing Plate

A plate was designed which would be mounted on top of the load sensing rings and which would support the wheel. (As mentioned previously, two such plate-and-ring assemblies can be placed side by side to accommodate dual wheels.) In previous tests on passenger vehicles made with Hamilton's drop beam, plate decelerations as high as seven g's were measured. These high decelerations were caused by the beam suddenly coming to rest after it had been dropped, and they gave rise to large inertia forces, due only to the mass and deceleration of the plate. The inertia forces were directly proportional to the weight of the load plate, and in some cases were almost as

large as the force variation being measured. These inertia forces introduced an error into the "transfer function" obtained from the calibration test. In order to minimize this error the weight of the load plate had to be reduced as much as possible since large decelerations are needed to provide the impulse that excites the suspension system of the vehicle.

Base and Installation

The weight of the beam and accessories was great enough to make a portable unit impractical. The beam was therefore designed to be mounted on a base, with the entire device recessed in the ground so that the top surface of the load plates was flush with the surface of the ground. With this arrangement, additional ramps or structures are not needed to support the other wheels.

CHAPTER 4

DESIGN OF PRINCIPAL COMPONENTS

The design of certain components of the truck calibrator required careful analysis. The rings for measuring the applied load were most critical in this respect. Careful design procedures were needed to select load ring dimensions which would enable the rings to meet all of the design specifications. The drop beam also required careful consideration. An attempt was made to make the beam very light, and yet very rigid. The wheel supporting plates used in the load cells were also designed to be very light and rigid. The following sections describe the design procedures used for each of the above components, and briefly indicate the design techniques used for the less critical elements of this device.

Load Ring Dimensions

As stated in Chapter 3, the following three criteria had to be considered in the design of the load rings:

1. The maximum stress occurring in the ring due to the maximum wheel load had to be well below the proportional limit.
2. The ring and plate assembly, when loaded with the maximum wheel load had to have a fundamental natural frequency well above any frequency excited in the vehicle during a test.

3. The strain sensitivity, or strain measured by the strain gages per pound of applied force had to be high enough so that sizeable strains would be produced by the expected forces.

The static wheel load of 14,000 pounds represents the load exerted on the beam by a set of dual wheels. Each load plate would therefore support a maximum static load of 7,000 pounds, and therefore each of the four rings supporting the plate must be designed for a maximum static load of 1,750 pounds.

The maximum stress occurring in a ring is at point "A" in Figure 7. and is equal to (8):

$$\sigma_a = \frac{M_a C}{I} = \left(\frac{P_{max}}{\pi} R\right)\left(\frac{h}{2}\right)\left(\frac{12}{bh^3}\right)$$

or

$$\sigma_a = \sigma_{max} = \frac{6 P_{max} R}{\pi b h^2} ,$$

Where:

P_{max} = maximum static load of 1,750 lbs. on each ring

R = mean radius of the ring

b = width of ring

h = thickness of ring

σ_{max} = maximum stress in ring, (located at point A)

I = area moment of inertia of the cross section of the ring at "A" about an axis perpendicular to the plane of the drawing. ($I = \frac{1}{12} bh^3$)

M_a = bending moment at "A"

C = distance from the neutral axis to the surface fiber of the ring

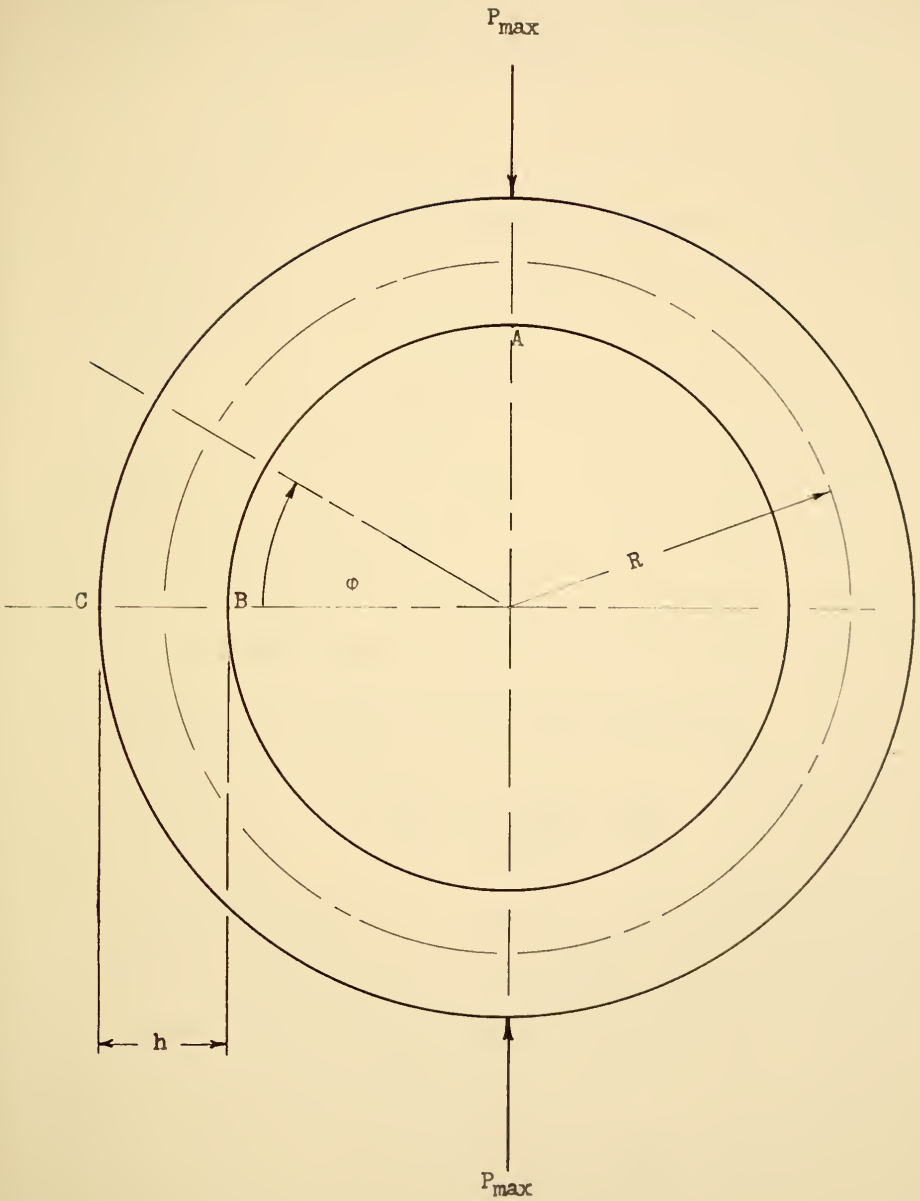

FIGURE 7: DRAWING OF FORCE MEASURING RINGS

Substituting the value of P_{max} into the previous equation, it becomes:

$$\sigma_{max} = 3340 \left(\frac{R}{bh^2}\right) \qquad (1)$$

To get an expression for the strain sensitivity, it is necessary to compute the strain at points "B" and "C" in Figure 7, since these are the points of application of the strain gages. The stress at point B, σ_b, due to a load P is:

$$\sigma_b = \frac{M_b C}{I} \pm \frac{P}{2A}$$

Where:

$M_b = .1817\ PR\ (15)$

$A = bh$

and other quantities are the same as previously defined.

Substituting values of I, M_b, C and rearranging:

$$\frac{\sigma_b}{P} = (1.09)\left(\frac{R}{bh^2}\right) \pm \frac{1}{2bh} \qquad (2)$$

Equation (2) above is an expression for the "stress per unit force" at the points of application of the strain gages. This can be changed into strain sensitivity by dividing by the modulus of elasticity E of the material from which the ring is made. This gives

$$\frac{\varepsilon_b}{P} = \left(\frac{1.09}{E}\right)\left(\frac{R}{bh^2}\right) \pm \frac{1}{2bhE}$$

The second term on the right hand side of this equation is much smaller than the other terms and therefore can be neglected for the present. The

"strain sensitivity per unit force" at point B is therefore approximately:

$$\frac{\varepsilon_b}{P} \approx \left(\frac{1.09}{E}\right)\left(\frac{R}{bh^2}\right) \qquad (3)$$

The load rings, wheel, and vehicle suspension system are actually a complicated elastic system having several degrees of freedom. A mathematical model of this system would be quite involved, and the parameters of the model would be different for different vehicles. Also, non-linearities in the vehicle suspension system would add additional complications. All of these factors make an accurate calculation of the fundamental natural frequency of the vehicle on the load plate and rings difficult. Some assumptions can be made, however, which facilitate the computation of a lower limit for this natural frequency.

If the static wheel load of 1,750 pounds per ring is assumed to be the weight of a mass concentrated on top of the ring, and the ring is considered as a linear spring, the natural frequency is:

$$f_n = \frac{1}{2\pi}\sqrt{\frac{kg}{P_{max}}} \qquad (4)$$

Where:

k = spring rate of the load ring

f_n = natural frequency of the loaded ring in cycles per second

P_{max} = load per ring as defined before

The natural frequency, f_n, calculated from the above relationship is either equal to or lower than the fundamental natural frequency of the loaded ring.

The deflection of the load ring in the direction of the load, δ, may be calculated by the Theorem of Castigliano (9) which gives

$$\delta = .149 \frac{PR^3}{EI}$$

Where P is the load applied to produce the deflection δ, and the other quantities are the same as previously defined.

The spring rate of the ring, k, is the load per unit deflection, or

$$k = \frac{P}{\delta}$$

Substituting values of δ and I, the spring rate becomes

$$k = \frac{E\left(\frac{1}{12} bh^3\right)}{(.149) R^3} ,$$

or

$$k = \frac{E\ bh^3}{1.79\ R^3} \tag{5}$$

Substituting equation (5) into equation (4), the lower limit value for the natural frequency f_n, becomes

$$f_n = \left(\frac{1}{2\pi}\right) \sqrt{\frac{E\ bg\ h^3}{(1.79)\ R^3\ P_{max}}} \tag{6}$$

Substituting the value of P_{max}, equation (6) can be written:

$$f_n = (.0559) \sqrt{\frac{E\ bh^3}{R^3}} \tag{7}$$

Equations (1), (3), and (7) are expressions of the three design criteria to be satisfied. It should be noted that the ring width, b, appears linearly

in equations (1) and (3). To reduce the number of parameters, b was arbitrarily selected to be 1.0 inch. This simplified the three equations to:

$$\frac{\sigma_{max}}{R} = \frac{3340}{h^2} \tag{8}$$

$$\left(\frac{\varepsilon_b}{P}\right) = \frac{(1.09)\,R}{E\,h^2} \tag{9}$$

$$\frac{f_n}{E^{1/2}} = \left(\frac{.0559}{R^{3/2}}\right) h^{3/2} \tag{10}$$

To determine usable dimensions for the rings, the above equations must be satisfied along with the following practical limitations:

1. $\sigma_{max} < 40{,}000$ psi, a safe working stress for steel or some aluminum alloys
2. $f_n > 45$ cycles per second
3. $\left(\frac{\varepsilon_b}{P}\right) \geq .58$ microinches per inch per pound of applied load (This sensitivity is the same as Hamilton's load cell, which is satisfactory.)
4. From a practical point of view, R should not be less than 1 inch, and not more than 3 inches.
5. The ratio $\left(\frac{R}{h}\right)$ should be as large as possible. If $\left(\frac{R}{h}\right)$ is greater than ten, thin ring theory holds very well (10).

Equation (8) was plotted on log-log paper in Figure 8. A line corresponding to $\sigma_{max} = 40{,}000$ lbs./square inch, R = 1 inch was drawn. The intersection of this line and the plot of equation (8) establish a lower limit on "h", - that is, h must be greater than .29 inches.

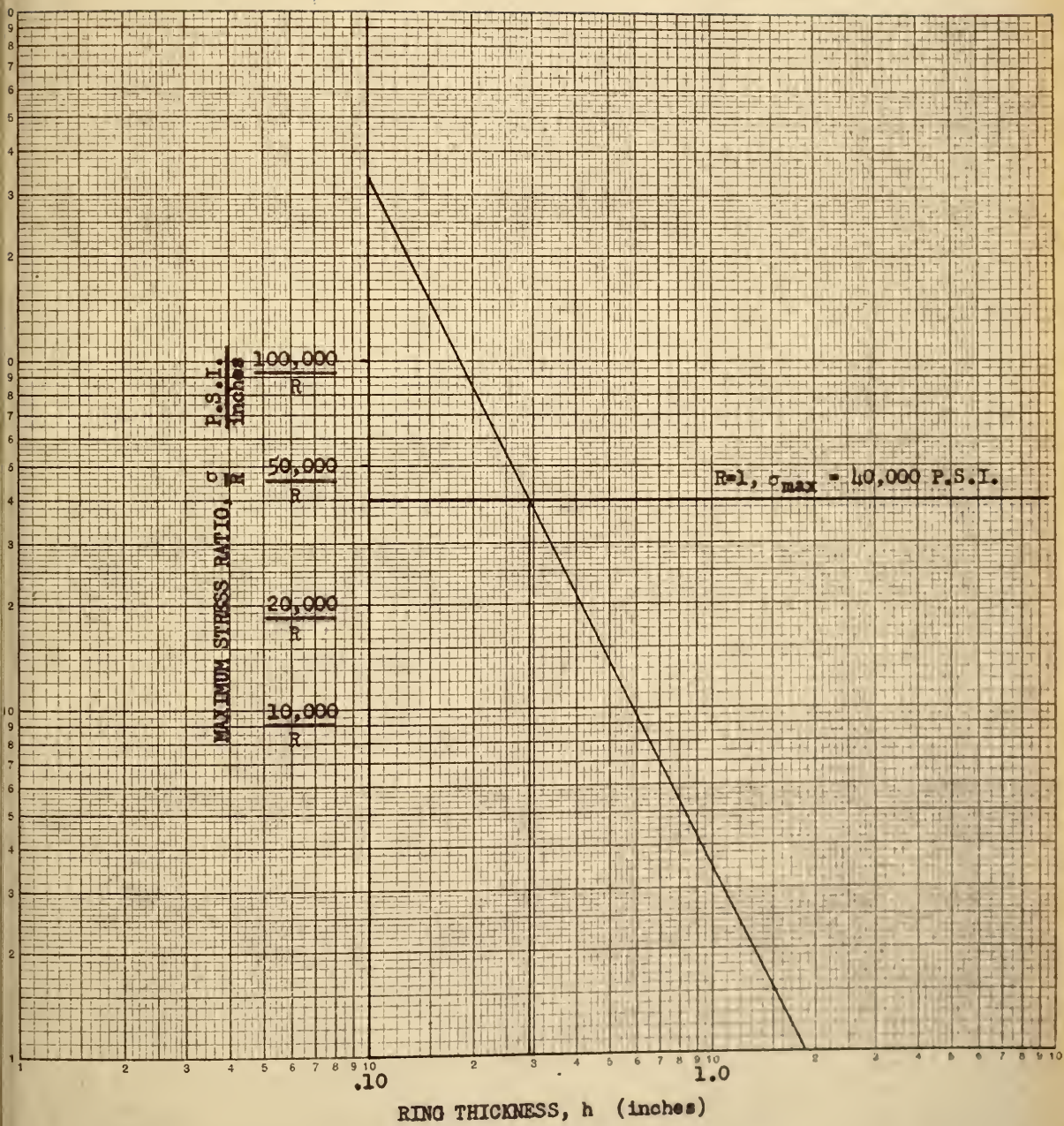

FIGURE 8: MAXIMUM STRESS RATIO VS RING THICKNESS

Next, equation (9) was plotted on log-log paper in Figure 9 for values of R from 1 inch to 3 inches and for values of E for steel and aluminum. A line corresponding to $\frac{\varepsilon_b}{P}$ = .58 microinches per inch per pound was drawn on Figure 9. An examination of Figure 9 shows that the intersection of the line $(\frac{\varepsilon_b}{P})$ = .58 and the plot of equation (9) for aluminum which has a modulus E of 10.5 x 10^6, and R = 3 inches puts an upper limit on "h". Only two of the original three criteria have been used, and h is bounded above and below:

$$.29" \leq h \leq .73"$$

Equation (10) was plotted as Figure 10. Lines corresponding to R = 1, R = 2, R = 3 were drawn. Lines corresponding to f_n = 45 cps for both aluminum and steel rings, and the upper and lower limits on h were also drawn. From Figure 10, it can be seen that the frequency limitation (45 cps or greater) and the upper limit on h restrict R in the following manner:

For aluminum rings: $1.0" \leq R \leq 1.8"$

For steel rings: $1.0" \leq R \leq 2.7"$

Re-examining Figure 9 for the effects of these limitations on R, it appears that the upper limit on h has been lowered. For aluminum rings, h cannot be greater than .56 inches, and for steel rings h cannot be greater than .4 inches.

Referring again to Figure 10 to determine the effects of these additional limitations on h, it can be seen that for either steel or aluminum rings the maximum allowable value of R has been reduced to about 1.5 inches. Figure 9 shows that if R is not greater than 1.5 inches, for steel rings, the upper limit on h has been further reduced to about .32 inches. For aluminum rings the upper limit on h has been reduced to about .50 inches.

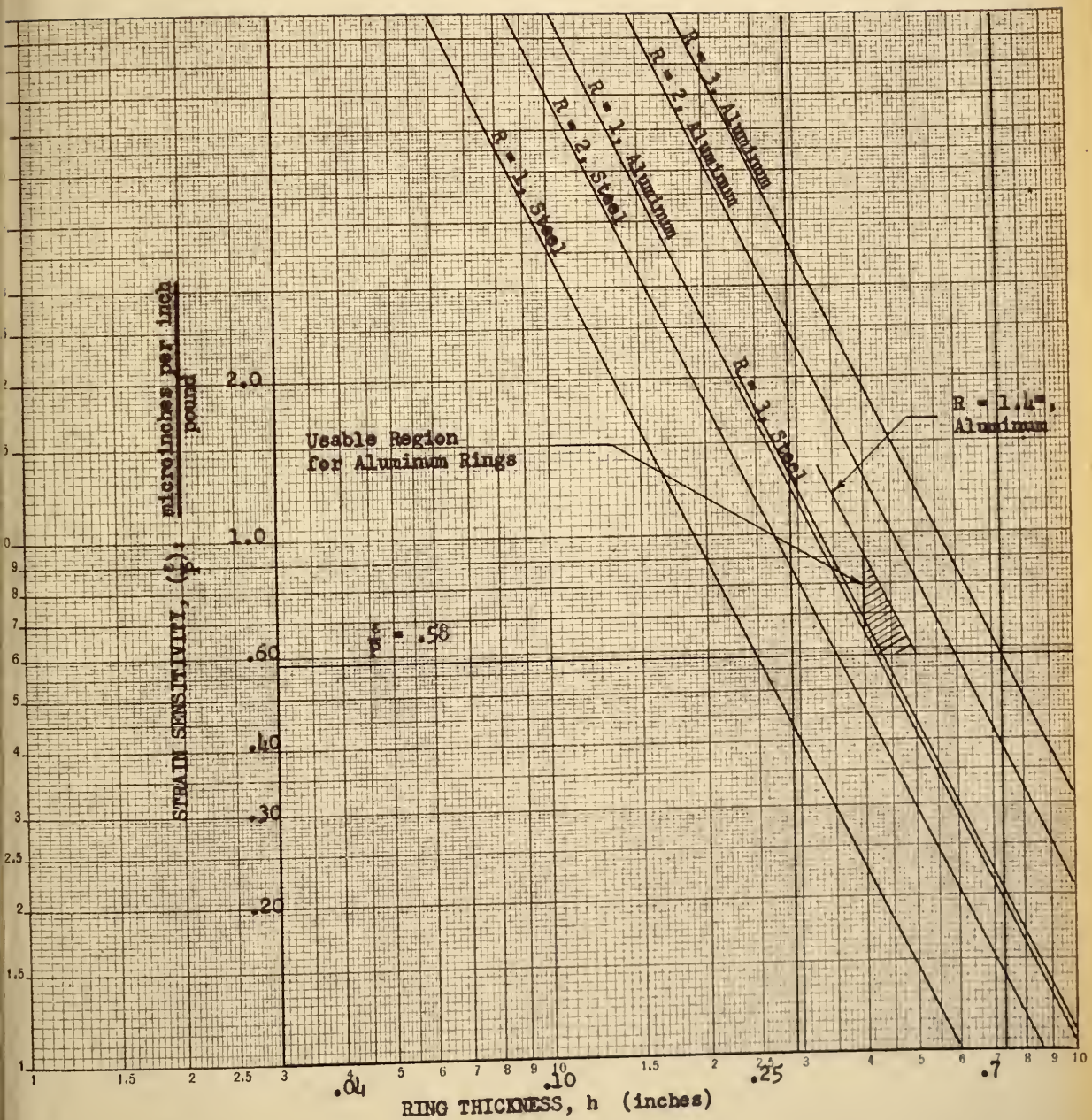

FIGURE 9: STRAIN SENSITIVITY VS RING THICKNESS

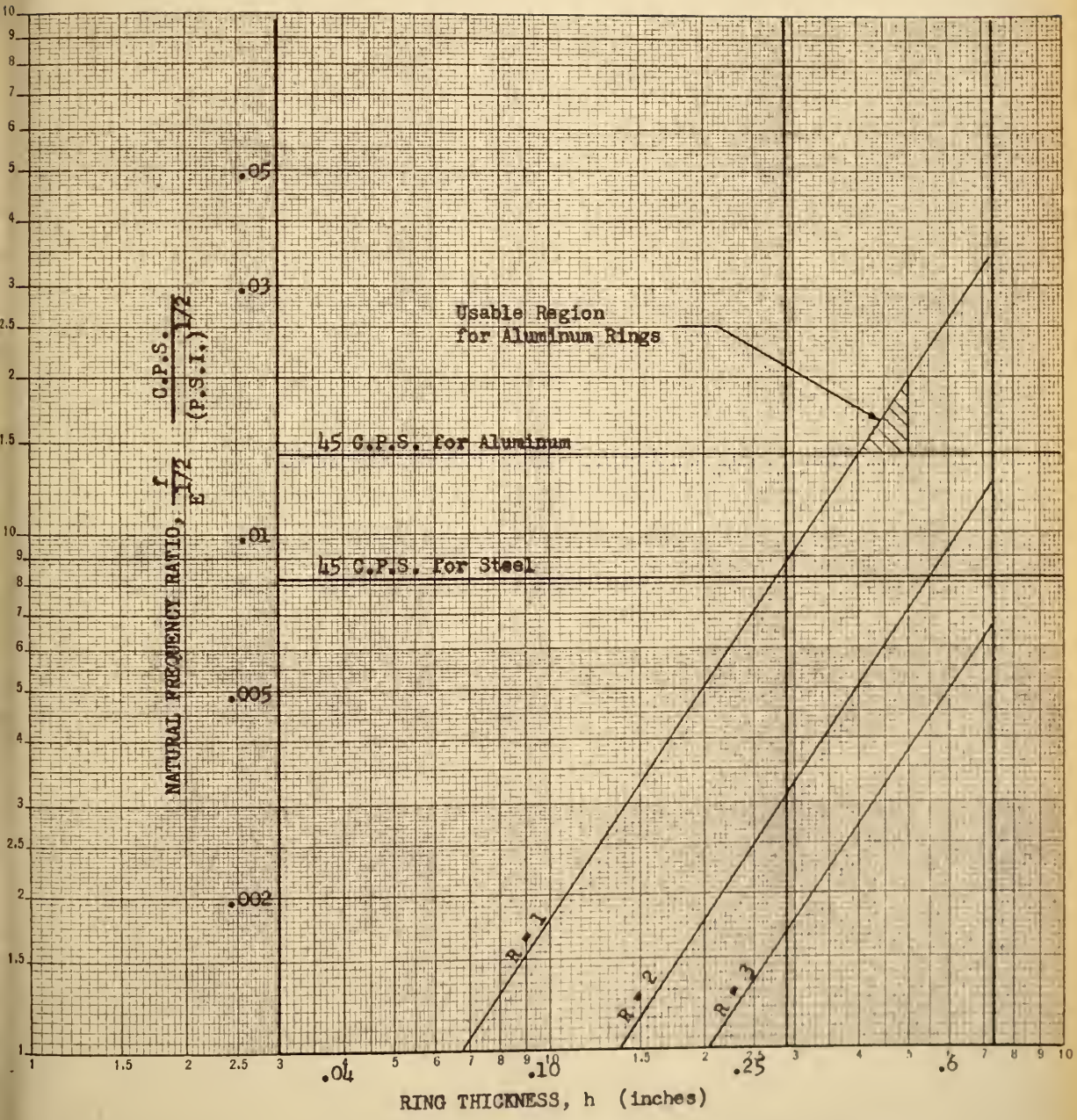

FIGURE 10: NATURAL FREQUENCY RATIO VERSUS RING THICKNESS

The shaded area on Figure 10 is the region containing parameters for aluminum rings which will satisfy the design specifications. It should be noted that there is no usable region for steel rings. When the upper limit on h was limited to .32 inches for steel rings, Figure 10 further limited the upper limit on R to about 1.2 inches. The sensitivity condition in Figure 9 then reduced the upper limit on h to approximately the same value as the lower limit, so that no usable region exists which will satisfy all of the design specifications.

Any point in the shaded area of Figure 9 which is also in the shaded area of Figure 10 will satisfy the design specifications. Points lying just outside of one of the shaded areas may be close enough to be usable.

Several possibilities were picked from the graphs and investigated. The graphical method was checked by substituting the selections into the original equations. Examples of sets of parameters which either satisfy, or very nearly satisfy the specifications are:

SET I

$R = 1.0"$

$h = .4"$

$f_n = 45.8$ cps

$\frac{\varepsilon}{P} = .65$

$\sigma_{max} = 20{,}900$ psi

$\frac{R}{h} = 2.5$

and

SET II

$R = 1.1"$

$h = .4"$

$f_n = 40.0$ cps

$\frac{\varepsilon}{P} = .714$ MI/lb.

σ_{max} = 23,000 psi

$\frac{R}{h}$ = 2.75

In both instances b is 1.0 inch and the material is 7075 T-6 Aluminum or 2024 T-4 Aluminum.

The second set of parameters was selected for the ring dimensions. While the natural frequency for these dimensions may be slightly low, the sensitivity is very good. Eight rings of this size were made from 2024 T-4 Aluminum alloy.

One minor discrepancy remains to be resolved. The thin ring theory used in the above design procedure contains errors introduced by the small value of the ratio $\frac{R}{h}$. If $\frac{R}{h}$ was two, there would be a 17 percent error introduced into the maximum stress calculation by using thin ring theory (11). To correct this error, the selected design parameters must be checked using thick ring theory.

Using thick ring equations (12), the maximum stress was computed to be 26,100 pounds per square inch rather than the 23,000 pounds per square inch value obtained from thin ring equations. The strain sensitivity is different at the inside and outside strain gage positions, but the strain sensitivity per ring (4 gages) is the same as that computed by thin ring equations. Therefore, the selected design is safe, and the sensitivity is slightly better than the value specified.

Load-Bearing Plate

As mentioned in Chapter 3, the load bearing plate must be as light as possible in order to reduce the inertia force measured by the load rings.

The original load plate used with Hamilton's load cell (3) was a homogeneous plate made of steel. When it became apparent that the weight of the load plate created a problem, an aluminum alloy plate of the same size was substituted for the steel plate. This reduced the weight by a factor of three, however it was felt that further weight reduction was needed, particularly in the design of the truck calibrator plates.

As an experimental design, a built-up plate was constructed for use with Hamilton's load cell. The plate was a laminated design consisting of two sheets of 24 ST aluminum alloy bonded on both sides of a 1 inch sheet of plywood with epoxy resin to form a sort of "sandwich". This plate was used extensively in calibration tests on passenger vehicles and served its purpose quite well.

The experimental plate described above had proved that the use of such a laminated plate was feasible. The same method of calculation used in the design of the experimental plate was then used to design load plates for the truck calibrator. The truck calibrator plates were constructed in much the same manner as the previous plate, but were built to support larger tires and greater loads. Design calculations are outlined in the following section.

Design Calculations

The following design assumptions were made:

1. The plate is homogeneous, isotropic, and simply supported.
2. Stresses and deflections can be calculated by considering the plate to be a beam of the same length and width.

3. The maximum static wheel load of 7,000 pounds per plate can be considered as a constant uniformly distributed load over the plate surface, since the tire print size at this force level is about the same size as the plate.

While the above assumptions are not entirely true, a large factor of safety was used to compensate for the uncertainty.

The required section modulus and moment of inertia were calculated. The aluminum plates were then designed so that by themselves they had the required moment of inertia. The plywood was used only as a filler to connect the two plates.

The equivalent beam is shown in Figure 11. The maximum moment occurs at the center, and is equal to 10,500 pound inches. The aluminum plates were made from 2024 T-4 alloy, which has a yield point stress, σ_{yp}, of 42,000 pounds per square inch. If a factor of safety of eight is used, the required section modulus is:

$$Z = \frac{M_{max}}{\sigma_w} = \frac{M_{max\ (F.S.)}}{\sigma_{yp}}$$

Where:

$Z = \frac{I}{c}$ = section modulus

σ_w = working stress

M_{max} = maximum moment of 10,500 pound inches

Substituting numerical values, the section modulus becomes:

$$Z = \frac{(10,500)(8)}{(42,000)} = 2.0\ (in.)^3$$

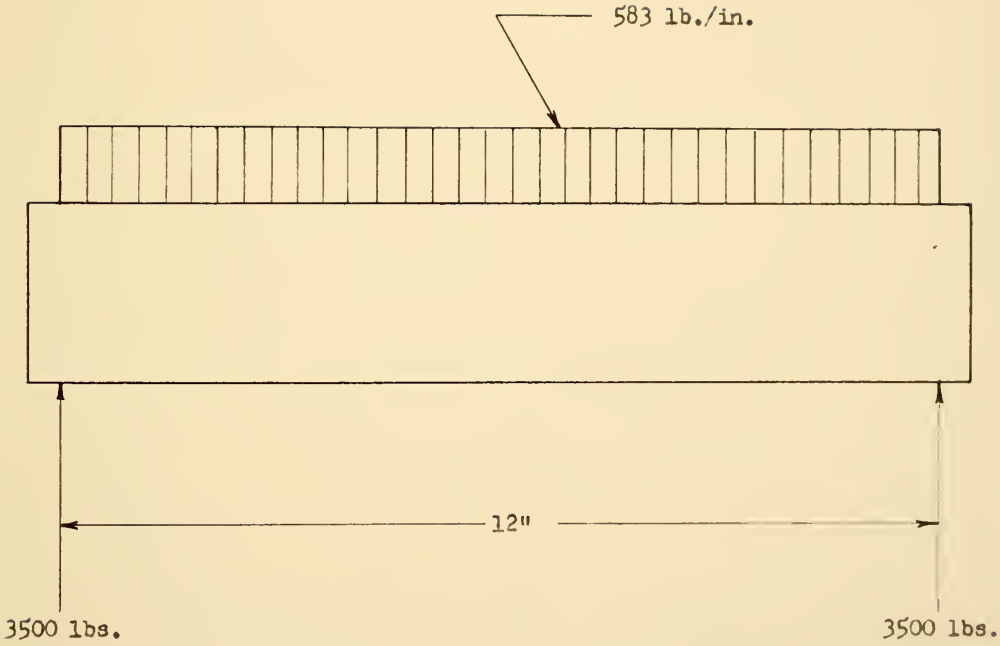

FIGURE 11: EQUIVALENT BEAM FOR LOAD PLATE

If aluminum plates .125 inches thick are used, the moment of inertia can be calculated: (See Figure 12)

$$I = 2 A d^2$$

Where:

A = cross sectional area of one aluminum plate,

d = distance from centroid of the aluminum plate to the neutral axis.

Substituting values:

$$I = (2)(8)(.125)[\frac{h - .125}{2}]^2$$

$$I = \frac{64 h^2 - 16 h + 1}{128}$$

But

$$I = \frac{h Z}{2} = h, \quad \text{therefore:}$$

$$h = \frac{64 h^2 - 16 h + 1}{128}, \quad \text{or}$$

$$64 h^2 - 144 h + 1 = 0$$

$$h = 2.25 \text{ inches}$$

The load plates were constructed using plywood 2 inches thick and two sheets of 2024 T-4 aluminum alloy having a thickness of .125 inches.

Drop Beam

As stated in Chapter 3, the drop beam must support a maximum static load of 14,000 pounds and an additional fluctuating force during a test. The beam must be wide enough to accommodate dual wheels. To reduce material

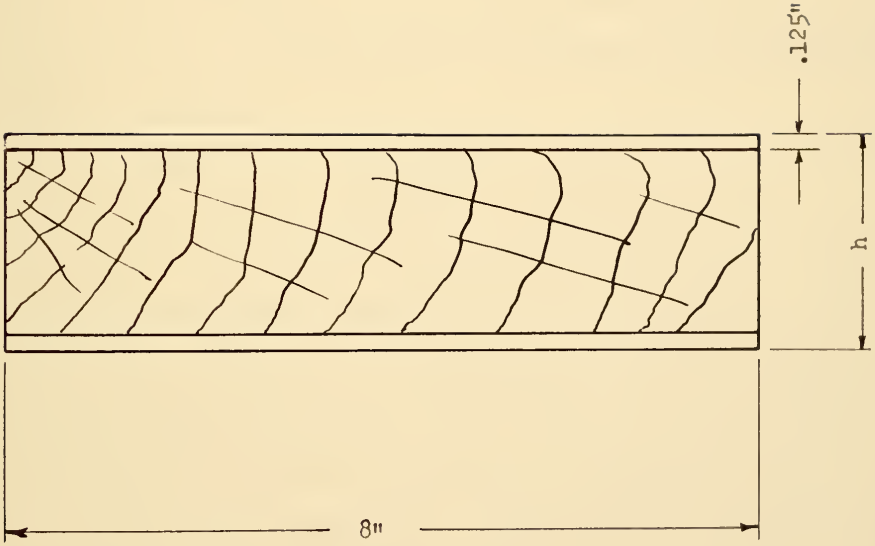

FIGURE 12: LOAD PLATE CROSS SECTION

costs, and facilitate assembly and use, the beam should be as light as possible. It should have no natural frequencies in the range of frequencies excited in a test.

The beam length was chosen to be six feet, or five feet six inches from pivot shaft center line to latch point. (Figure 6) If the beam was longer, it would not be as stiff. It could not be much shorter than the chosen length because of the tire size. Also, a shaft was inserted through the moving end of the beam, the center line of which is five feet from the center line of the pivot shaft. This shaft was intended for use with a driving mechanism if such a mechanism is added. (A suggested driving mechanism is described in Chapter 6.)

The beam width was selected to be thirty inches. This is just about the minimum width which can comfortably accommodate dual wheels.

The cross section of the beam was designed in the form of a built-up section, made of thin sheet steel. This was done in an attempt to get as stiff a beam as possible with as little weight as possible. (While the beam has been repeatedly referred to as a "beam", the length and width dimensions given above make it seem that the beam should correctly be called a "plate".) With this cross-section, a large area moment of inertia can be obtained with a minimum amount of metal.

Beam Natural Frequency

Calculation of the fundamental natural frequency of the loaded beam would be difficult, however a frequency can be calculated which will be equal to or lower than the lowest natural frequency. This can be done by making the following assumptions:

1. The assumptions of elementary strength of materials and linear elasticity hold (13).
2. The beam is simply supported, with a span length of five and one half feet.
3. The beam supports a concentrated load at the center equal to the static wheel load of 14,000 pounds. (See Figure 13.)

With these assumptions, no natural frequency could be lower than:

$$f = \frac{1}{2\pi} \sqrt{\frac{kg}{w}}$$

Where:

k = spring rate of a simply supported beam

W = static wheel load of 14,000 pounds

g = acceleration of gravity

For a simply supported beam with a concentrated load at the center, the spring rate is:

$$k = \frac{48\ E\ I}{l^3}$$

Where:

l = length of span, five and one half feet

I = area moment of inertia of the section

E = modulus of elasticity of the material

The lower limit on the natural frequency is therefore:

$$f = \frac{1}{2\pi} \sqrt{\frac{48\ E\ Ig}{W\ l^3}} \qquad (11)$$

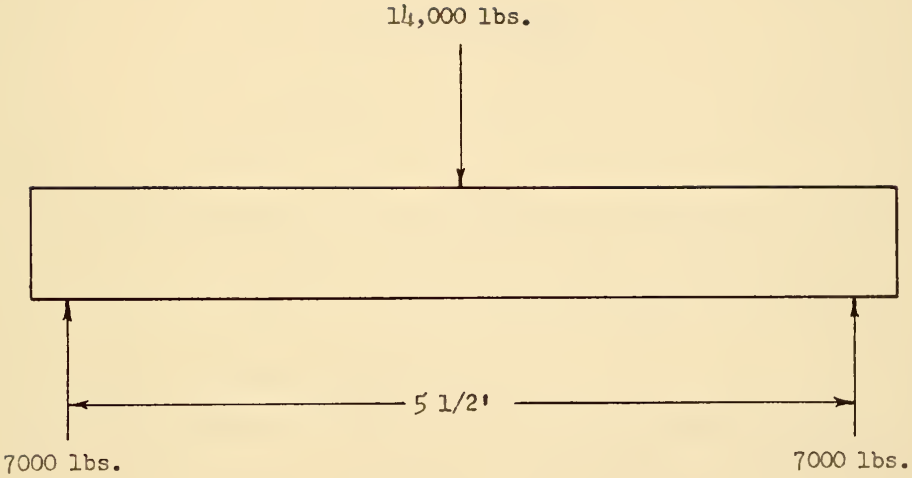

FIGURE 13: SKETCH OF DROP BEAM LOADING

By rearranging equation (11), the moment of inertia necessary to establish this lower limit is

$$I = \frac{\pi^2 f^2 W l^3}{12 E g} \qquad (12)$$

If a lower limit for the natural frequency, f, is chosen to be fifty cycles per second and other numerical values are inserted, I becomes:

$$I = \frac{\pi^2 (50)^2 (14{,}000)(66)^3}{(12)(30 \times 10^6)(386)}$$

$$I = 714 \text{ in.}^4$$

The above calculations show that in order to guarantee that the beam has no natural frequency below 50 cycles per second it must have an area moment of inertia of 714 $in.^4$. Wheel sizes also require it to have the length and width previously mentioned.

The required moment of inertia could have been obtained by using standard structural members, but because the beam must be 30 inches wide, several members would be needed to support the bearing load on top of the beam and to guard against bending of the beam in the transverse direction. Obviously, the beam can be made as stiff as desired by putting a greater quantity of steel into it. The number of structural members needed would make the beam extremely heavy. In view of this, a light gage cold formed steel section seems to have distinct advantages.

The design of light gage steel structural members has been extensively treated in the literature.(14). In the reference cited, specifications are given for the design of many types of sections. In the design of the drop

beam, however, the combination of bending and concentrated bearing loads makes some type of internal cross bracing necessary if light gage steel is to be used. A schematic drawing of the drop beam cross section and the method of bracing used is shown in Figure 14. Such a cross section is not specifically treated in the above reference.

The internal bracing is needed to support the bearing load on the beam even if it does not contribute to the resistance to bending. There is some doubt as to just what part of the total cross section can be considered as contributing to the effective moment of inertia. For stiffened light gage members (14), design specifications state that the design should be based on a reduced, or "effective" width. However, as previously pointed out, the specifications do not treat the type of bracing used in the drop beam. If the effective width is applied to the outer shell of the beam, (assuming that the bracing does not offer any resistance to bending.) The moment of inertia computed from the reduced section is about 110 $in.^4$. (See Figure 15). If the diagonal braces are considered as running longitudinally and the entire cross section is considered as effective, then the minimum moment of inertia encountered throughout the beam length is about 700 $in.^4$, which is very nearly equal to the required moment of inertia that was calculated.

For design purposes, it was assumed that the entire cross section contributed to the effective moment of inertia, and that the effective moment of inertia was 700 $in.^4$. This assumption was made with full realization of the uncertainties involved. In the next section, it will be shown that steps were taken to reduce the effects of these assumptions.

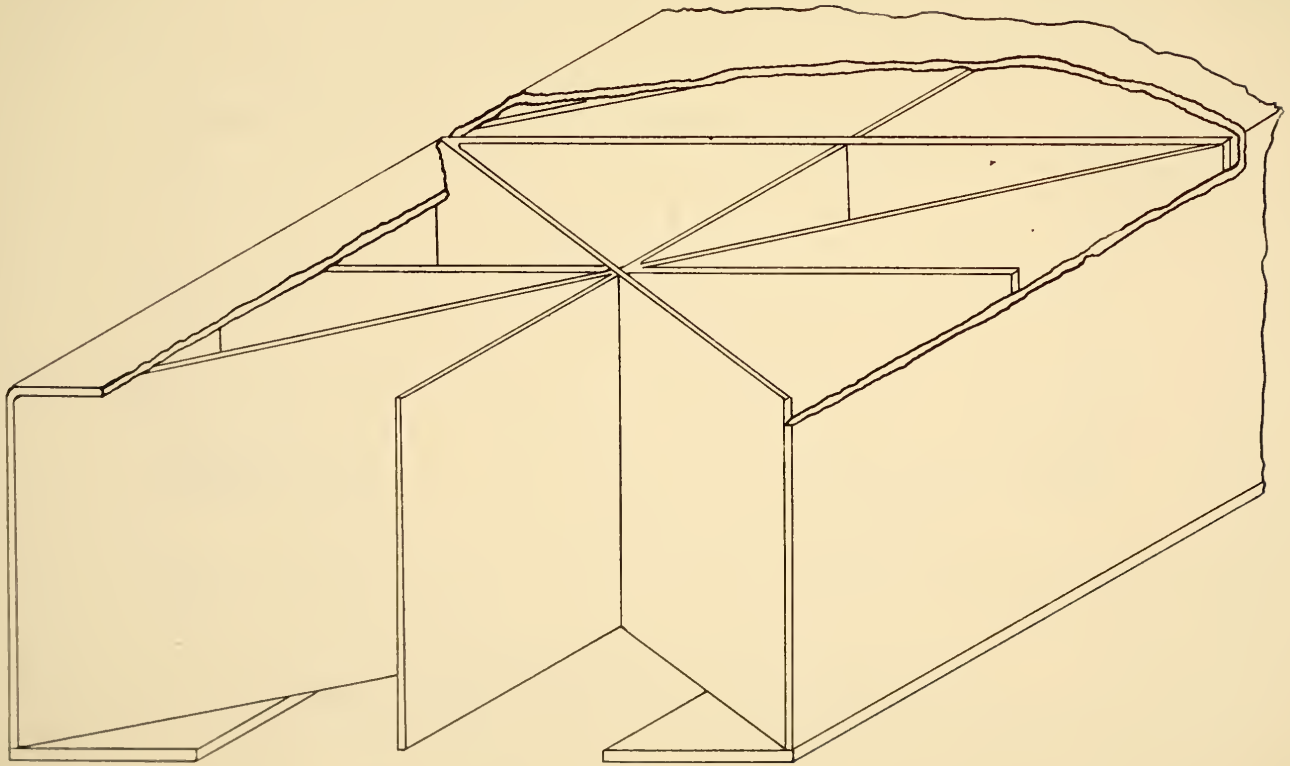

FIGURE 14: ISOMETRIC DRAWING OF BEAM CROSS SECTION SHOWING METHOD OF BRACING

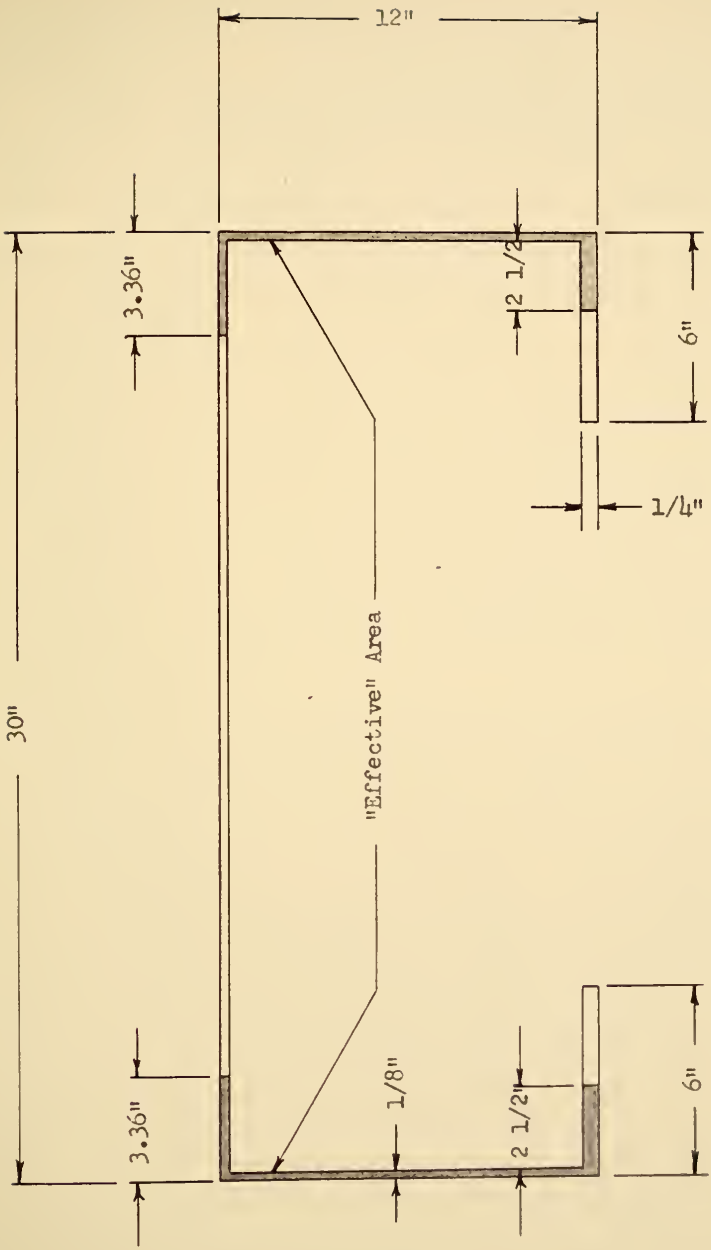

FIGURE 15: REDUCED OR "EFFECTIVE" CROSS SECTIONAL AREA

Base, Pit, and Assembly

There is considerable uncertainty regarding the effective moment of inertia of the beam. Because of this uncertainty, the base on which the beam is mounted was designed in such a way as to make the beam stiffness less critical. In Figure 6, it can be seen that when the beam bottoms in a drop test it bottoms on the base over three-fourths of the length. This prevents first mode vibrations from occurring. As an additional precaution, the beam also bottoms on sheets of foam rubber. The rubber acts as a damping material to assist in damping out higher mode vibrations.

The entire base and beam assembly was mounted in a pit. Concrete flooring and walls 6 inches thick were constructed in a pit with inside dimensions of 8 feet by 10 feet by 39 inches deep. The base was bolted to the concrete floor.

The beam pivot shaft was mounted in self-aligning sleeve bearings on the base. The modular load cells were mounted on top of the beam and are easily removable. Wooden runways on top of the beam make the top of the beam level with the top of the load plates. (See Figure 6.)

An adjustable latch bracket on the moving end of the beam makes it possible to adjust the drop height. When the beam is raised, a pivoted latch engages the latch bracket to hold up the beam. For a drop test, the latch is pulled out, allowing the beam to fall.

CHAPTER 5

TEST RESULTS

Several components of the calibrator were tested in the Structures Laboratory of the Civil Engineering School. The following sections describe the tests performed, and compare the test results with predictions.

Test of Load-Bearing Plates

The two load-bearing plates were mounted on rings in the same manner in which they will be used. The assembly was placed in a testing machine and a force was applied to the plate. The force was applied over an 8 inch by 12 inch area, since this is the approximate size of the tire print when the tire supports a load of 7,000 pounds.

The plates were designed for a static load of 7,000 pounds. They must also support a dynamic load. The test machine used was capable of exerting only a static force, so to simulate the more extreme operating conditions, static forces far in excess of 7,000 pounds were applied.

Both plates were loaded up to 10,000 pounds several times. Each time when the load was removed they were examined and no visible damage could be seen.

One plate was loaded to 15,000 pounds in an attempt to determine the maximum load that it would support. Between ten and 15 thousand pounds, cracking sounds were heard, and it could be seen that the epoxy resin was cracking away from the edges. At 15,000 pounds, a slight deflection at the center could be visibly detected, and the corners of the aluminum plates

had separated from the plywood. When the load was removed, no permanent set could be seen in the plate, and the only apparent damage was the cracked epoxy. This test yielded a very important observation: although the plate was loaded to more than twice the static load for which it was designed and most of the epoxy had cracked away, it still supported the load. The plate was repaired by re-cementing with epoxy, and was once again serviceable.

After the test, one slight modification was made on the plates. Eight one-fourth inch bolts were inserted through each plate, one at each corner and one half way between each two corners near the edge. It was felt that these bolts would carry part of the stress on the cement between the plate and the plywood, and at the same time prevent separation at the corners.

Calibration of Load Rings

After the load cells were assembled in final form, a test quite similar to the one described in the previous section was used to calibrate the load sensing rings.

There are four strain gages on each of four rings supporting a load plate. The 16 gages constituting one load cell were connected as shown in Figure 16 to form a four-arm bridge. The strain sensitivity was calculated in Chapter 4 to be .714 microinches per inch per pound of force applied to the ring for each gage. In the test, a force was applied to the plate. The force on the plate was varied from zero up to 7,000 pounds, and the strain per gage was recorded at 500 pound force increments. A curve of Strain (per gage) versus Force Applied to a ring is shown in Figure 17. (The force exerted on one ring is one-fourth of the force exerted on the plate). The slope of this curve is the strain sensitivity as it was defined

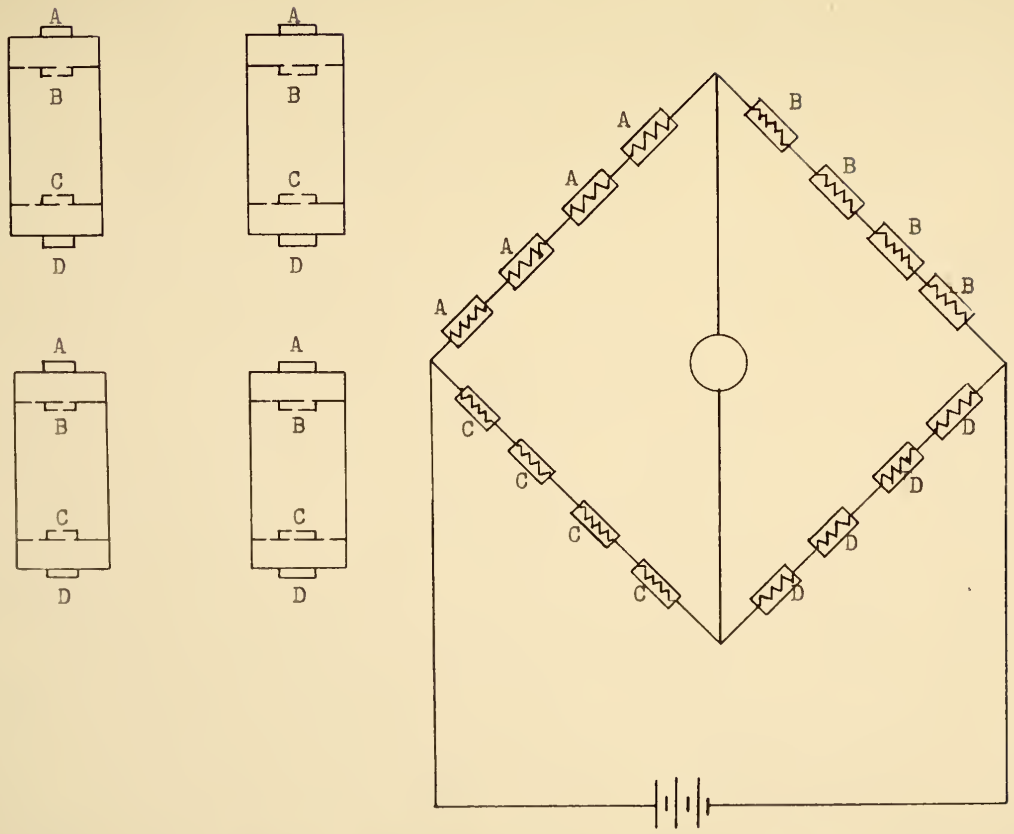

FIGURE 16: BRIDGE CIRCUIT FOR FORCE MEASURING RINGS

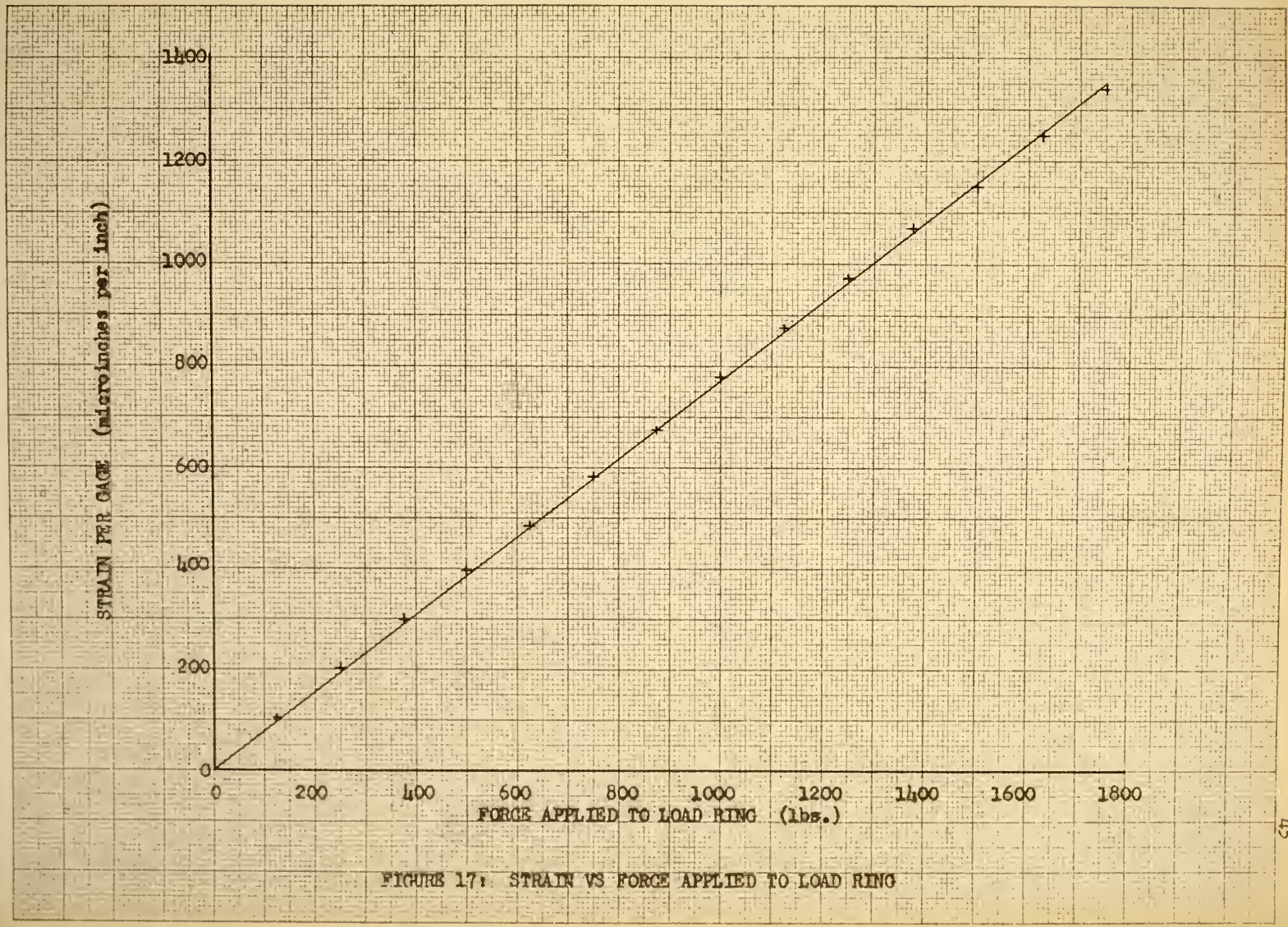

FIGURE 17: STRAIN VS FORCE APPLIED TO LOAD RING

in Chapter 4. The measured sensitivity for one gage was .756 microinches per inch per pound which is within six percent of the predicted value.

Force - Deflection Measurement for Drop Beam

The drop beam was tested to determine the actual beam stiffness. A force was applied at the center of the beam and the deflection was measured under the beam on each side, and on top at the load head. The curves of Force versus Deflection that were obtained are shown in Figure 18.

The slope of the curves was found to be:

$$k = 5.33 \times 10^5 \text{ pounds per inch}$$

The measured spring rate can be converted to an effective moment of inertia, I_{eff} by

$$I_{eff} = \frac{k\,l^3}{48E} = \frac{(5.33 \times 10^5)(60)^3}{(48)(30 \times 10^6)}$$

$$I_{eff} = 80 \text{ in.}^4$$

The effective moment of inertia is actually much less than the moment of inertia of the full section, and even slightly less than the value calculated by the effective area method (14). This indicates that the internal bracing contributes virtually no resistance to bending, and that the effective area method described in the specifications (14) is only approximate.

The failure to achieve the desired beam stiffness is not as alarming as it may seem. As pointed out in Chapter 4, the manner in which the beam is supported after it is dropped makes the beam stiffness much less critical than if the beam were supported at each end after the drop.

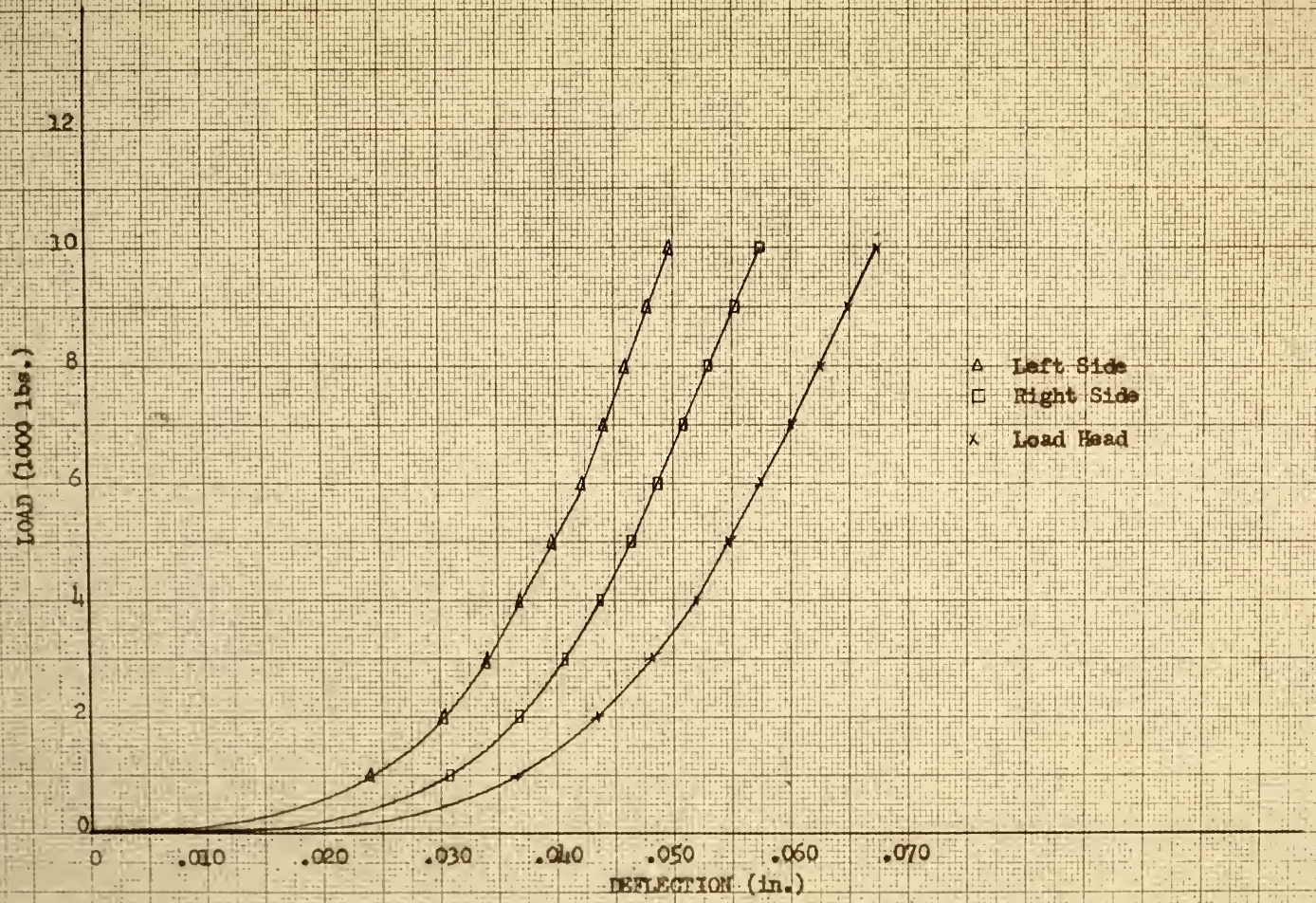

FIGURE 18: LOAD VS DEFLECTION FOR TRUCK DROP BEAM (WITH CHANNELS)

CHAPTER 6

CONCLUSIONS AND RECOMMENDATIONS

As a consequence of the test results and observations made on the completed components of the truck calibrator, the following conclusions were reached:

1. The design specifications for the load rings could not be satisfied with steel rings, however, 2024 T-4 aluminum alloy rings satisfied the conditions reasonably well.
2. The design procedure used in selecting the load ring dimensions proved to be very workable. Measured strains agreed closely with predicted strains. The semi-graphical technique described in Chapter 4 offers a systematic approach to this complicated problem.
3. The laminated plates performed well under test. The design technique used was approximate, but an exact analysis of the behavior of non-homogeneous plates is difficult and therefore a large factor of safety was used with the simpler analysis. The "sandwich" type of construction is economical and can be used in other applications where light weight and low cost are important.

4. The AISI specifications (14) were followed closely and the beam design was structurally satisfactory. The desired stiffness was not fully realized, however. The design of the base and the method for supporting the beam are such that the beam stiffness is less critical than originally anticipated.
5. Internal cross bracing in the beam was needed to support the bearing loads, but it contributed relatively little resistance to longitudinal bending.
6. The adjustable latch bracket makes it possible to vary the drop height. Drop heights up to three-fourths of an inch (at the load cell) can be achieved.

Recommendations

The following recommendations are suggested for operating the calibrator:

1. The static wheel load should never exceed 7,000 pounds per load cell plate.
2. The following parts should be lubricated as specified:
   a. The three bearings on the beam pivot shaft should be lubricated with light oil.
   b. The two bearings on the latch pivot shaft should be lubricated with light oil.
   c. Heavy chassis grease should be used on the two latch surfaces: the adjustable latch bracket, and the mating surface on the latch.

3. No one should be in the pit during a drop test.
4. Load cells should be removed and stored indoors when the calibrator is not in use.

As previously discussed, the drop beam will be released from an elevated position with one wheel of a vehicle in position on the load plate. The impulse resulting from the rapid deceleration of the beam as it comes to rest will produce a transient motion in the suspension system of the vehicle. By analyzing this motion the frequency domain characteristics of the vehicle can be determined.

Future research may indicate that it is also desirable to raise and to lower the moving end of the drop beam in a prescribed manner in order to produce a different transient motion in the vehicle. Certain provisions for doing this have already been built into the calibrator and the pit in which it is mounted is already large enough to accommodate the additional equipment. The driving mechanism to raise and lower the beam can be mounted on a separate base or can be attached to the present structure.

A suggested driving mechanism is shown schematically in Figure 19. It consists of a toggle mechanism actuated by a double-acting piston and cylinder. A storage tank of compressed air, or compressed nitrogen provides the driving force. A small quantity of the high pressure fluid is bled into the intermediate tank. The quick-opening valve at "A" is then opened causing the piston to drive to the right. The tie rod, "C", pulls the toggle mechanism over center, producing both the rise and fall of the moving end of the beam. Pre-charging of the cylinder at "B" can control the deceleration of the piston. Preliminary calculations indicate that standard piston and cylinder devices are on the market which can easily be utilized.

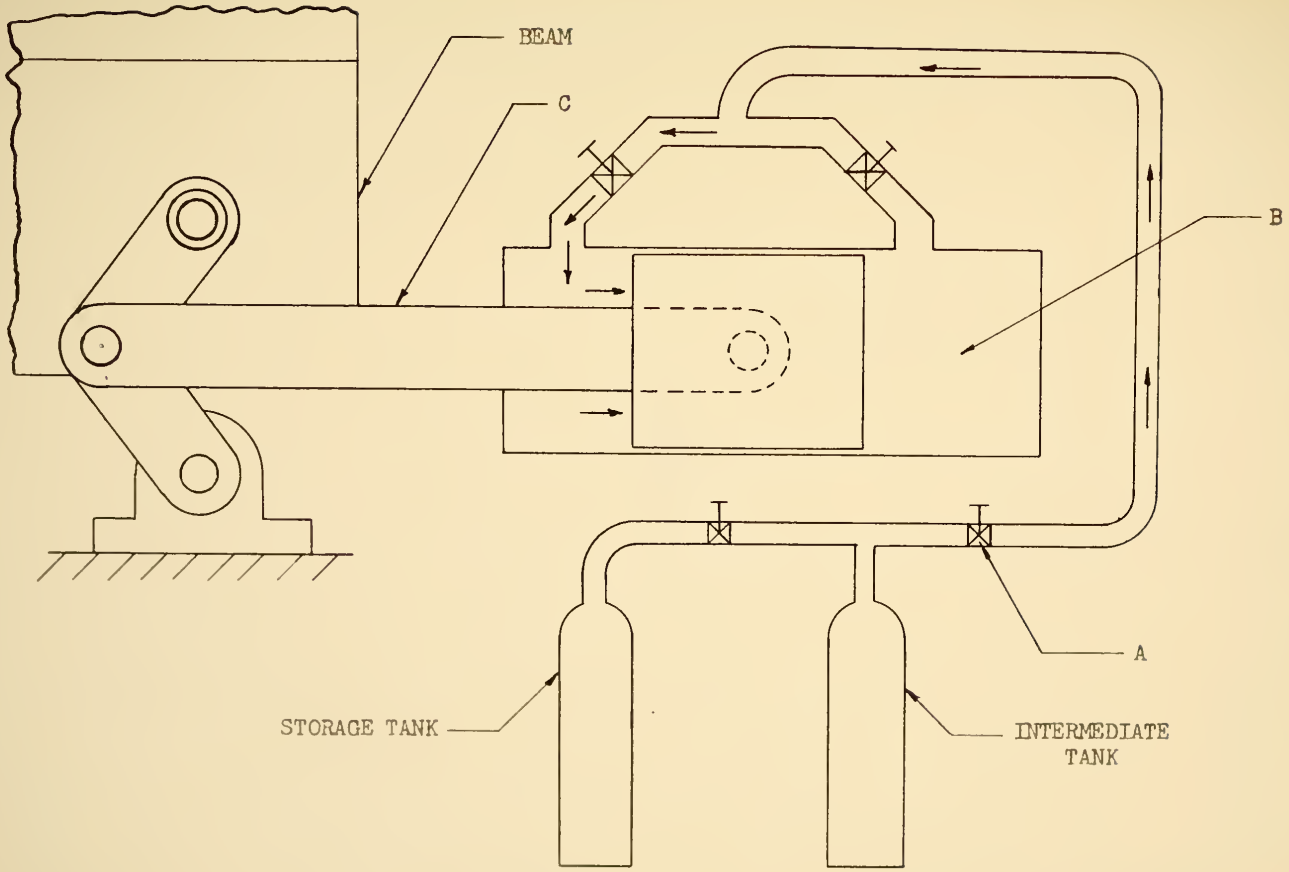

FIGURE 19: SCHEMATIC DRAWING OF PROPOSED DRIVING MECHANISM FOR PRODUCING PULSE INPUT

BIBLIOGRAPHY

BIBLIOGRAPHY

1. De Vries, Thomas W., "A Statistical Method for Estimating Dynamic Vehicle Loads on Highways," Purdue University, Ph.D. Thesis, January 1961.

2. Emmerson, Calvin W., "A Study of Tire Pressure as Related to Dynamic Vehicle Reactions," Purdue University, MS Thesis, January 1963.

3. Hamilton, James F., "Determination of Vehicle Characteristics Influencing Dynamic Reactions on Highways," Purdue University, Ph.D. Thesis, August 1963.

4. Hopkins, R. C. and Boswell, H. H., "Methods for Measuring Load Transfer through Vehicle Tires to the Road Surface," Highway Research Board, Proceedings, Volume 36, 1957.

5. Levenick, R. L., "Measurement of Pavement Impact Loading," Report Number PG-8740, Copy Number 30, October 24, 1957, Experimental Engineering Department, General Motors Proving Ground.

6. Quinn, B. E. and Van Wyk, R.,"A Method for Introducing Dynamic Vehicle Loads into Design of Highways," Proceedings, Highway Research Board, Volume 40, 1961.

7. SAE Report of Joint Subcommittee on Tractor-Trailer Ride, May 24, 1956.

8. Timoshenko, S., Strength of Materials, Part I, D. Van Nostrand Co., Inc., page 379, 1955.

9. Timoshenko, S., Strength of Materials, Part I, D. Van Nostrand Co., Inc., page 381, 1955.

10. Timoshenko, S., Strength of Materials, Part I, D. Van Nostrand Co., Inc., page 369, 1955.

11. Timoshenko, S., Strength of Materials, Part I, D. Van Nostrand Co., Inc., page 370, 1955.

12. Seely, Fred B. and Smith, James O., Advanced Mechanics of Materials, second edition, John Wiley and Sons, Inc., New York, page 180, 1952.

13. Cox, G. N., Germano, F. J., Bateman, J. H., Strength of Materials, Pitman Publishing Corporation, page 134, 1951.

14. Light Gage Cold-Formed Steel Design Manual, American Iron and Steel Institute, 1962.

15. Roark, Raymond J., Formulas for Stress and Strain, third edition, McGraw-Hill Book Company, Inc., New York, 1954.